Resonant spin flavor precession constraints on neutrino parameters and solar magnetic fields from solar neutrino data

B. C. Chauhan, U. C. Pandey,* and S. Dev
Department of Physics, Himachal Pradesh University, Shimla-171005, India
(Received 17 July 1998; published 12 March 1999)

The resonant spin flavor precession (RSFP) constraints on neutrino parameters have been updated in light of the latest solar neutrino data. The standard solar model, in spite of its enormous success in predicting the thermal and nuclear evolution of the Sun, is unable to throw enough light on solar magnetic activity. In the absence of a reliable theory of the solar dynamo believed to be responsible for solar magnetic activity and insufficient astrophysical data on solar magnetic activity, it may be worthwhile to constrain the solar magnetic fields from the solar neutrino observations assuming the RSFP to be responsible for the solar neutrino deficit and the possible time variation of solar neutrino flux. The configuration of the solar magnetic field consistent with the solar neutrino observations has been derived and found to be in reasonably good agreement with the distribution proposed by Akhmedov and Bychuk [Sov. Phys. JETP **68**, 250 (1989)]. However, this work ruled out the magnetic field distribution in the radiation zone used by Pulido [Phys. Rep. **211**, 187 (1992)]. The magnitude of the magnetic field in the radiation and the convective zone of the Sun are very sensitive to the value chosen for the neutrino magnetic moment. [S0556-2821(99)02204-3]

PACS number(s): 26.65.+t, 13.40.Em, 14.60.Pq, 96.60.Hv

INTRODUCTION

Neutrinos are the by-products of thermonuclear reactions occurring deep inside the solar core. Because of their extremely weak interactions with matter, the neutrinos provide a real time window into the processes going on in the solar interior. All the solar neutrino experiments report of deficit of neutrino flux compared with the predicted neutrino fluxes [1]. Moreover, the most recent solar neutrino data [2] from the ongoing experiments with different energy windows on the solar neutrino spectrum reveal a serious discrepancy in the relative neutrino fluxes from different steps of the *pp* chain. A reduced flux of boron neutrinos has been observed but hardly any beryllium (^{7}Be) neutrinos have been observed. However, ^{8}B cannot be produced without producing ^{7}Be in the previous step of the chain. In fact, the ^{7}Be neutrino flux is the second best predicted flux in the standard solar model (SSM) and the ^{7}Be neutrino flux predictions from different models have only a 10% spread. The ^{7}Be neutrino flux is far less sensitive than the ^{8}B neutrino flux to changes in the solar interior. But the recent solar neutrino data reveal that the deviation of the ^{7}Be neutrino flux from the SSM prediction is larger than that of ^{8}B neutrino flux. This situation almost completely rules out an astrophysical solution of the solar neutrino problem. This total suppression of ^{7}Be neutrinos is revealed by a comparison of Kamiokande results with the Homestake experiment results and independently with the results of GALLEX and SAGE. The ^{8}B neutrino flux is about 0.41 times the flux predicted by the SSM. The low-energy *pp* neutrino flux, on the other hand, is the least suppressed. This differential suppression of the solar neutrino spectrum forces us to seek the solution of the solar neutrino problem in terms of nonstandard neutrinos.

The main neutrino physics solutions of the solar neutrino problem (SNP) are based on neutrino oscillations, neutrino decay, and neutrino magnetic moments. The most elegant solution of SNP is the one proposed by Mikheyev, Smirnov, and Wolfenstein (MSW) [3] and is in good shape. Neutrino decay solution has already been ruled out as it predicts a stronger depletion of the lower-energy neutrino flux in contradiction with the data. Another attractive solution proposed by Okun, Voloshin, and Vysotsky (OVV) [4] is based on a possible large neutrino magnetic moment for the electronic neutrino. However, the OVV mechanism cannot account for the differential suppression of the different components of the solar neutrino spectrum. Another variant of OVV mechanism was proposed by Lim and Marciano [5] and independently by Akhmedov [6] (LMA) in which spin-flavor precession is resonantly enhanced by matter effects. The suppression rate of electronic neutrinos in the LMA scenario depends on neutrino energy whereas it is independent of neutrino energy in the OVV scenario. Since an energy-dependent suppression of solar neutrino flux is indicated by the solar neutrino data, we intend to work within the framework of the LMA scenario even though the time variation of the solar neutrino flux with the solar magnetic activity has neither been conclusively confirmed nor ruled out by the solar neutrino observations. The time structure of the low statistics Homestake data hints to an anticorrelation with solar magnetic activity whereas Kamiokande data show little or no time variation. However, the apparent lack of time variation in the Kamiokande data can be explained by noting that the Kamiokande is only sensitive to high-energy neutrinos and, moreover, for Majorana neutrinos, the LMA mechanism converts ν_{el}, into $\overline{\nu}_{\mu R}$ or $\overline{\nu}_{\tau R}$ which do contribute to the Kamiokande event rate through comparatively smaller neutral current cross sections which results in a reduced amplitude of time variation of the neutrino signal in Kamiokande and, thus, explains the difference between the time variation

*Permanent address: Indira Gandhi National Open University, A-24, Durga Chembers Distt. Centre Raj Nagar, Ghaziabad, (U.P.), India.

of the neutrino signal observed by the Homestake and the Kamiokande experiments. GALLEX and SAGE, on the other hand, have not observed any statistically significant time variations of the neutrino signal. However, the lack of time variations of the neutrino signal in gallium experiments can be naturally explained within the RSFP framework if the magnetic field in the radiation zone of the solar core where the low-energy neutrinos, which constitute a major part of the neutrino signal in gallium detectors undergo RSFP conversion, is not too strong. This is because the inner magnetic field is unknown but it does not vary in time. The high statistics super-Kamiokande on the other hand, has been in operation for too short a period to confirm or disprove any time variations of the neutrino signal. Thus, the different degrees of suppression and the time variation or lack thereof of the solar neutrino flux observed by all the ongoing solar neutrino experiments can all be explained by the RSFP of the electronic neutrinos as a result of their magnetic moment interactions with the solar magnetic field even though the requisite neutrino magnetic moment is several orders of magnitude larger than the standard model prediction for the same.

Raichoudhury [7] has analyzed the solar neutrino data through the first and the second maxima of the solar cycle. The table below [7] presents the average solar neutrino detection rate through the first sunspot maximum (June 1989) to second sunspot maximum (May 1992) from all the solar neutrino experiments in operation at that time.

	Sunspot maximum	
	I	II
HOMESTAKE	2.20 SNU	4.32 SNU
	(June 1989 to April 1990)	(May 1991 to May 1992)
KAMIOKANDE	$=0.40\pm0.09$	$=0.60\pm0.15$
	(June 1989 to April 1990)	(Jan. 1991 to Aug. 1991)
SAGE	40 SNU	109 SNU
	(Jan 1990 to July 1990)	(July 1991 to Aug. 1991)
GALLEX		92 SNU
		(May 1991 to April 1992)

It is clear from the table above that all the four ongoing solar neutrino experiments suggest that the neutrino flux observed at the time of the first sunspot maximum is significantly different from the flux observed during the second sunspot maximum. In fact, the neutrino flux observed during the second sunspot maximum is consistently and significantly higher than that observed during the first sunspot maximum. Raychoudhury [7] has also ruled out a constant neutrino flux observed by Kamiokande throughout the solar cycle using parametric as well as nonparametric methods. Others claiming a time variation of the solar neutrino flux include Oakley *et al.* [8] and Massati *et al.* [9].

More recently, two other groups have suggested the use of a more local indicator of the solar magnetic activity to study its correlation with the solar neutrino signal since the sunspot number, in their opinion, is too gross a feature of the solar magnetic activity. One of the groups used the direct surface measurements of the solar magnetic field strength along the line of the neutrino signal and found the correlation coefficient to increase significantly. The other group chose the green corona line as an indicator of the solar magnetic activity and found the anticorrelation between the green corona line and the Homestake signal to be much stronger for neutrinos emitted in the southern solar hemisphere than in the northern hemisphere. This conclusion has also been supported by Stanev [10]. This situation finds a natural explanation within the framework of the RSFP scenario with twisting magnetic fields. These and other related developments have been discussed in detail by Akhmedov [11].

I. THE MODEL

If $\Phi(E)$ is the neutrino flux predicted by the SSM and $\sigma(E)$ the corresponding cross section for interaction with the detector, the neutrino detection rate should be given by

$$R_{\mathrm{SSM}}=\int \Phi(E)\sigma(E)dE, \tag{1.1}$$

where the cross section $\sigma(E)$ obviously depends on the detection process. Since all the ongoing solar neutrino experiments report a deficit of neutrinos and the suppression, as discussed earlier, appears to be energy dependent, we introduce an energy-dependent suppression function $P(E)$ to bridge the gap between the predicted and the actually observed rates so that the observed rate is given by

$$R_{\mathrm{obs}}=\int P(E)\sigma(E)\Phi(E)dE. \tag{1.2}$$

Since all the ongoing solar neutrino experiments report neutrino deficits so $P(E)$ may be interpreted as the survival probability of electronic neutrinos in the RSFP scenario [12]. The RSFP occurs because of nonvanishing neutrino-transition magnetic moments which imply lepton flavor vio-

lation. As a result neutrino oscillations would invariably occur and one must, in general, consider the combined effect of the RSFP and neutrino oscillations. However, in this work the effects of neutrino mixing have been neglected. Because of their magnetic moment interactions with the transverse magnetic fields in the solar interior, the neutrinos with transition magnetic moments will experience spin rotation along with a flavor change. Here we assume the neutrinos to be Majorana particles. However, the probability of spin-flavor precession is suppressed in vacuum but the matter effects can enhance this probability resonantly. In the RSFP scenario, the propagation of neutrinos in solar matter is considered to be adiabatic except for a small region in the vicinity of the resonance centered at

$$r_{\rm res}=0.09R_s\log_e\left[\frac{5.02\times10^{-11}\ \text{eV}}{\Delta m^2_{21}/E}\right]. \tag{1.3}$$

Here R_s is the solar radius and $\Delta m^2_{21}=m^2_2-m^2_1$ and E is the neutrino energy. Assuming a linear density falloff along the nonadiabatic region, the crossing probability under the Landau-Zener approximation is given by

$$P_{LZ}=\exp\left[\frac{-\pi 2\mu^2B^2}{\Delta m^2_{21}/2E}0.09R_s\right] \tag{1.4}$$

and the total transition probability incorporating both adiabatic and nonadiabatic effects is given by

$$P_{\rm trans}=\frac{1}{2}-\left(\frac{1}{2}-P_{LZ}\right)\cos 2\tilde{\theta}_0\cos 2\tilde{\theta}_1, \tag{1.5}$$

where $\tilde{\theta}_0$ and $\tilde{\theta}_1$ are the respective mixing angles at the beginning and at the end of the neutrino trajectory. For the expected values of Δm^2_{21} and the magnetic field strength $\cos 2\tilde{\theta}_0\cos 2\tilde{\theta}_1\sim 1$, the total transition probability is given by

$$P_{\rm trans}=\exp\left(-\pi\frac{2B^2\mu^2}{\Delta m^2_{21}/2E}0.09R_s\right). \tag{1.6}$$

The SSM of Bahcall and Pinsonneault [1] is taken as the reference SSM here and confronted with the latest solar neutrino data in the following section to derive constraints on the neutrino parameters and the solar magnetic fields. The neutrinos are assumed to be produced at a distance of 35 000 km from the solar center and exponential falloff

$$GNe=2.11\times10^{-11}\exp(-r/0.09R_s)\ \ \text{eV}$$

of matter density is assumed where G is the Fermi constant and Ne is the number density of electrons.

II. THE RSFP CONSTRAINTS ON NEUTRINO PARAMETERS

The latest solar neutrino data are summarized by the following:

$$R_{\rm Cl}=0.32\pm0.03,$$

$$R_{\rm Ga}=0.56\pm0.07, \tag{2.1}$$

$$R_{\rm K}=0.51\pm0.07.$$

We recall that the chlorine experiment detects both the boron neutrinos as well as the beryllium neutrinos but the Kamiokande detects only boron neutrinos. In the gallium experiments, on the other hand, *pp* neutrinos account for 54%, boron neutrinos for 11%, beryllium neutrinos for 27%, CNO neutrinos for 6%, and the $p+e^-+p$ (pep) neutrinos account for 2% flux so that one can write

$$0.54x_{pp}+0.27x_{\rm Be}+0.02x_{\rm pep}+0.06x_{\rm CNO}+0.11x_B =0.56\pm0.07, \tag{2.2}$$

where x_i are the ratios of the observed and the predicted fluxes for $i=pp$, Be, B, pep, CNO, etc. Since Kamiokande detects only the boron neutrinos, we take

$$x_B=0.51\pm0.07.$$

A comparison of the chlorine and the Kamiokande experiments yields [13]

$$x^{\rm min}_{\rm Be}=0.0\quad\text{and}\quad x^{\rm max}_{\rm Be}=0.20(95\%\ \ \text{C.L.}). \tag{2.3}$$

In an energy-dependent suppression scenario, we take all the intermediate energy neutrinos to be equally suppressed so that $x_{\rm Be}\approx x_{\rm pep}\approx x_{\rm CNO}\cdots$. Thus Eq. (2.3) combined with Eq. (2.2) yields the lower and upper limits $x^{\rm max}_{pp}=0.93\pm0.13$ and $x^{\rm min}_{pp}=0.80\pm0.13$. So we conclude that the survival probabilities for different categories of electronic neutrinos must lie in the range

$$0.80<P_{pp}<0.93,$$

$$0.44<P_B<0.58, \tag{2.4}$$

and since a comparison of the chlorine and the Kamiokande experiments yields a negative value for the beryllium neutrino flux, the most probable value of the survival probability for beryllium neutrinos is taken to be zero. We performed a model calculation of survival probability in the RSFP scenario for a neutrino magnetic moment $\mu_\nu=10^{-11}\mu_B$ where μ_B is the Bohr magneton and taking the Akhmedov [14] model of the magnetic field profile in the solar interior given by

$$B(x)=\begin{cases}B_1[\gamma/(\gamma+x)]^k, & 0\leqslant x\leqslant 0.65,\\ B_0\left[1-\left(\dfrac{x-0.7}{0.3}\right)^2\right], & 0.65<x\leqslant 1,\end{cases} \tag{2.5}$$

where $x=r/R_s$ and $k=2$, $\gamma=0.2$. We considered almost all the possibilities for B_0 and B_1 and found that only for $B_0=3.6$ T and $B_1=220$ T the solar neutrino data summarized in Eq. (2.4) can be naturally explained in the RSFP scenario. This aspect is clearly brought out in Fig. 1. It is clear from the figure that $\Phi_{\rm Be}/\Phi_B$ flux anomaly along with the observed *pp* flux is well explained for

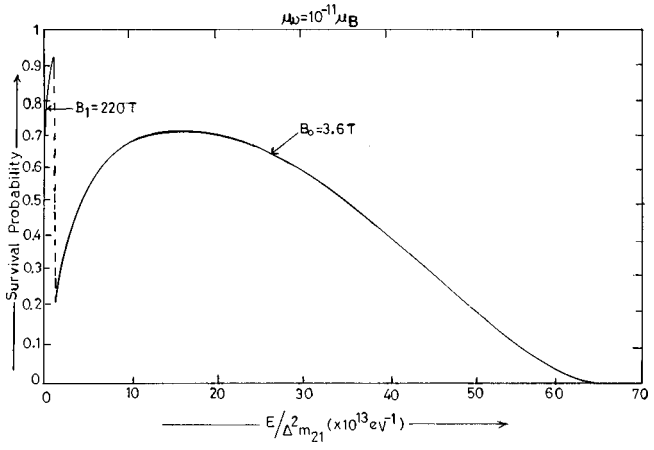

FIG. 1. Survival probability $v/s'E/\Delta^2_{m_{21}}{}'$ for a model magnetic field profile.

$$0.23\times10^{-7}\ \text{eV}^2 \leqslant \Delta m^2_{21} \leqslant 43.4\times10^{-7}\ \text{eV}^2 \qquad (2.6)$$

which is rather restrictive [15].

In Fig. 2, the constant probability curves for different categories of neutrinos have been plotted on a $(\mu_\nu, \Delta m^2_{21})$ plane for the model magnetic field profile proposed by Akhmedov [14] with $B_0 = 3.6\,\text{T}$ and $B_1 = 220\,\text{T}$ and the crossing region is obtained for

$$0.95\times10^{-7}\ \text{eV}^2 \leqslant \Delta m^2_{21} \leqslant 2.55\times10^{-7}\ \text{eV}^2$$

and

$$1.3\times10^{-11}\ \mu_B \leqslant \mu_\nu \leqslant 1.7\times10^{-11}\mu_B \qquad (2.7)$$

which gives the latest update on the neutrino parameters in the RSFP scenario in light of the latest solar neutrino data. These constraints on neutrino parameters are an order of magnitude more restrictive than the constraints derived by Pulido [16] which read as follows:

$$1.3\times10^{-8}\ \text{eV}^2 \leqslant \Delta m^2_{21} \leqslant 4.6\times10^{-8}\ \text{eV}^2,$$

$$2.3\times10^{-12}\mu_B \leqslant \mu_\nu \leqslant 4.6\times10^{-12}\mu_B. \qquad (2.8)$$

It is interesting to see that the bounds on the neutrino parameters $(\mu_\nu, \Delta m^2_{21})$ derived in Eq. (2.7) are within the qualitative range derived from Fig. 1.

III. THE RSFP CONSTRAINTS ON SOLAR MAGNETIC FIELDS FROM SOLAR NEUTRINO DATA

The RSFP in the solar interior introduces four additional astrophysical parameters into the analysis of solar neutrino data. These are the magnitude and extent of the magnetic fields in the convective and the radiation zones. These astronomical parameters can not be determined with confidence from the available astronomical data. Almost all our knowledge of solar magnetic fields is based on surface measurements. The solar surface is very rich in magnetic activity. It is currently believed that the solar magnetic fields are generated by a dynamo process at the interface between the convective zone and the radiative cores.

The main component of the solar magnetic field is toroidal with opposite polarities in the northern and southern solar hemispheres. The field certainly exists in the convective zone and may extend down to the core. The convective field is somehow caused by the rotation of the Sun (solar dynamo) and protrudes through the surface at the sunspots which are giant magnetic flux holes. At the sunspot maximum, the surface fields may reach 10^3–10^4 G inside the spots and then extend far out in the solar atmosphere where they produce flares and prominences, while at the sunspot minimum, the field falls below 10^2 G. Below the surface to the bottom of the convective zone, however, little is known about the mag-

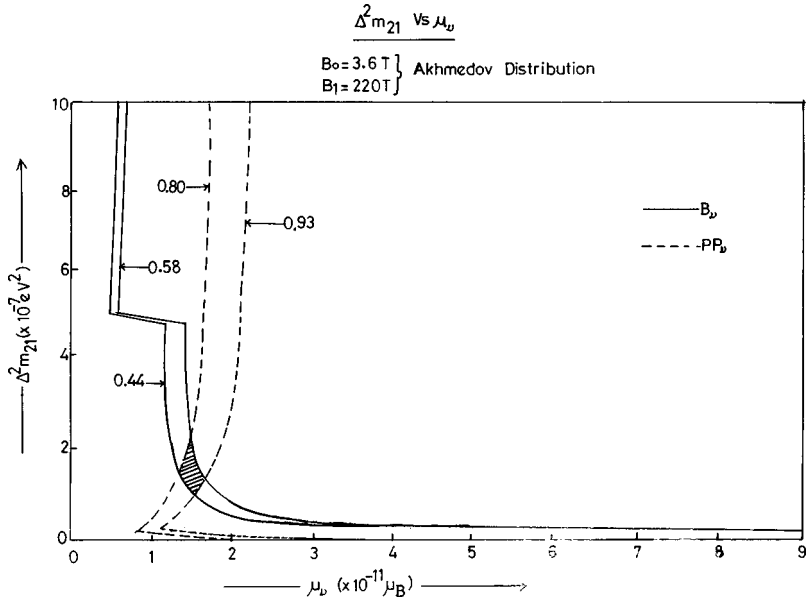

FIG. 2. Shaded area is the region of common parameter space $(\Delta m^2_{21}, \mu_\nu)$ consistent with the solar neutrino data.

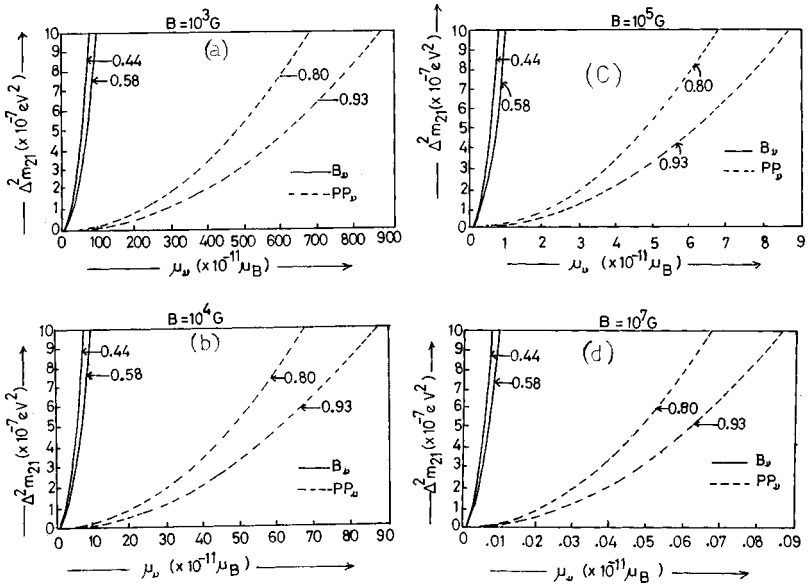

FIG. 3. Constant probability curves for constant magnetic fields in the $(\Delta m^2_{21}, \mu_\nu)$ space.

netic field except for an upper limit of 10^5 G from helioseismology. Large scale convective stability implies here a more stringent limit of 10^4 G. Below the convective zone, the magnetic field could be large but the field response time due to plasma effect is of the order of 10^{10} yr in this region [17]. Such a field if it exists will remain frozen over the entire life history of the Sun and would not be affected by the solar cycle. The configuration and the strength of the solar magnetic fields have been inferred from observations of the surface magnetic activity which is very complex and dynamical [18]. Even though, the SSM is fairly successful in predicting the thermal and nuclear evolution of the Sun, it throws little light on solar magnetic activity [19]. In the absence of a generally accepted theory of the solar dynamo, various general arguments have been put forth to constrain the magnetic fields in the solar interior. Parker [18], for example, has shown that a magnetic field in excess of 0.5×10^8 G in the central core would be lost from the Sun during its evolution as a consequence of its buoyancy. On the other hand, magnetic fields smaller than 10^9 G in the solar core or smaller than 10^7 G in the convective zone will hardly influence the thermal and nuclear evolution of the Sun which will still be well described by the SSM. It has been argued [20] that the nonlinear effects, which must limit the growth of the magnetic fields created by the dynamo process, constrain the convective zone magnetic field strength to be less than 10^4 G as larger fields will certainly exclude the turbulent motions and force the convective zone to recede further upwards which will suppress the further growth of the field. Parker and others [21] have shown that a strong field of the order of 4×10^5 G extending 3×10^4 km at the bottom of the convective zone would force the convective zone to extend deep enough to sufficiently destroy the ^{7}Li abundance though not completely destroying it during 4.5×10^9 yr of its evolution. Whether there exists a strong field in the radiation zone is still an open question. The only thing we can surmise is that if it exists, it will not show any periodicity because of the stable structure of the solar radiative core. The solar acoustic oscillations (p modes) can be used to infer the existence of extremely strong magnetic fields inside the Sun. Existing observations [19] place an upper limit of 10^7 G on the interior field which is within three orders of magnitude of the value required for the spin flip. In the absence of the reliable knowledge of solar magnetic fields from the available astrophysical data, it may be useful to constrain the solar magnetic fields from the solar neutrino observations within the framework of RSFP scenario.

To bring out the magnetic field profile dependence of RSFP, the constant probability curves on a $(\mu_\nu, \Delta m^2_{21})$ plane can be drawn for a few model magnetic field profiles used extensively in the literature [16]. As an example, we first consider a constant field in the production region and extending through the radiation and convective zones. For the survival probabilities of low and high energy neutrinos, we take

$$0.80 < P_{pp} < 0.93,$$

$$0.44 < P_B < 0.58,$$

and the survival probabilities of intermediate energy neutrinos to be zero. The resulting constant probability curves on a $(\mu_\nu, \Delta m^2_{21})$ plane for magnetic field magnitudes ranging between 10^3 to 10^7 G have been displayed in Fig. 3, assuming a linear density fall off along the nonadiabatic region (the Landau-Zener approximation). The constant probability curves do not cross for any constant value of the magnetic field so that there is no $(\mu_\nu, \Delta m^2_{21})$ parameter space consistent with the solar neutrino data for a constant magnetic field in the solar interior. Thus a constant magnetic field profile in the solar interior is conclusively ruled out by the solar neutrino data. We next consider another solar magnetic field profile used extensively [16] in connection with the RSFP of neutrinos. We take a constant field of 10^5 G extending through the core and radiation zones and decreasing linearly

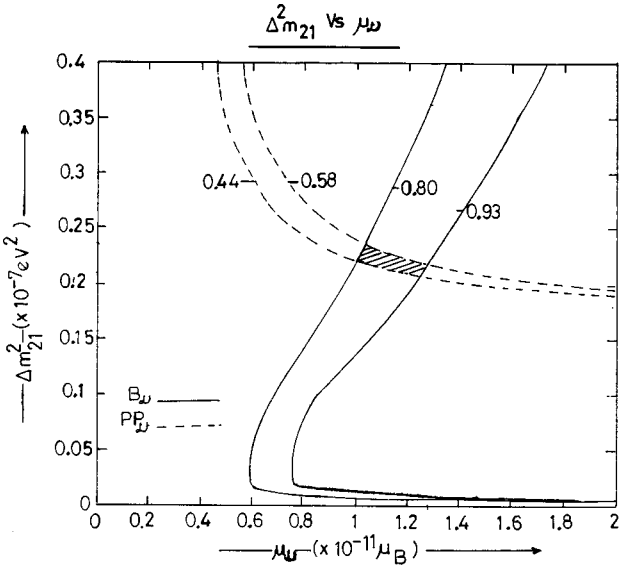

FIG. 4. Common parameter space for the linearly decreasing magnetic field in the convective zone of Sun.

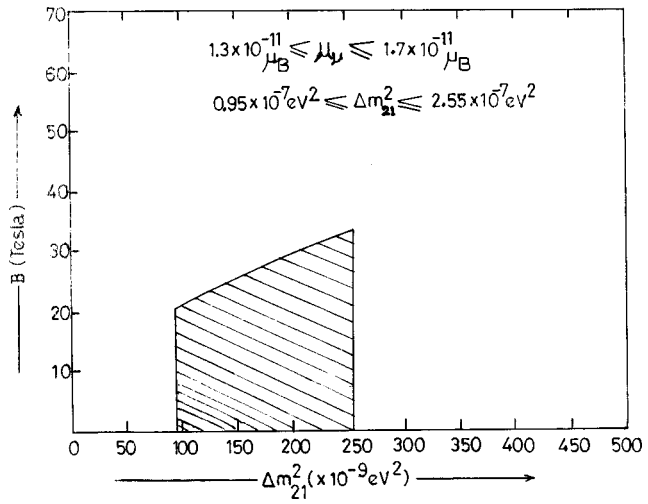

FIG. 5. $(B,\Delta m^2_{21})$ parameter space consistent with the latest solar neutrino data.

over the convection zone and reaching 10^2 G at a distance of $r=6.96\times10^5$ km from the solar centre. Assuming the borderline between the radiation and convective zones at $r=5\times10^5$ km, the field is given by

$$B=10^5 \text{ G}; \quad r\leqslant 5\times10^5 \text{ km},$$

$$B=10^5[1-5.26\times10^{-6}(r-5\times10^5)]; \quad r\geqslant 5\times10^5 \text{ km}, \tag{3.1}$$

where the distance is measured in km and the magnetic field in the units of G. The constant probability curves for this profile on a $(\mu_\nu,\Delta m^2_{21})$ plane have been drawn in Fig. 4 which yields a small common region of $(\mu_\nu,\Delta m^2_{21})$ parameter space consistent with the available solar neutrino data:

$$0.21\times10^{-7} \text{ eV}^2\leqslant\Delta m^2_{21}\leqslant 0.24\times10^{-7} \text{ eV}^2$$

$$10^{-11}\mu_B\leqslant\mu_\nu\leqslant 1.3\times10^{-11}\mu_B, \tag{3.2}$$

which is rather restrictive. The constant probability curves for the Akhmedov distribution (2.5) for the solar magnetic field have already been discussed in Sec. II and the resulting parameter space consistent with the available solar neutrino data is given in Eq. (2.7). One can also find out the required range of transverse solar magnetic field for RSFP to explain the available solar neutrino data for the range of Δm^2_{21} and μ_ν, obtained in Eq. (2.7). The results are shown in Fig. 5. This gives us the following range of the solar magnetic field:

$$0.17 \text{ T}\leqslant B\leqslant 33.6 \text{ T}, \tag{3.3}$$

which can explain the solar neutrino data within the framework of the RSFP model.

Since low, intermediate as well as high-energy neutrinos undergo flux suppression as evidenced by different solar neutrino experiments sensitive to different neutrino energies one can assume that all these categories of neutrinos undergo RSFP somewhere within the Sun which leads to the bound

$$1.15\times10^{-5} \text{ eV}^2>\Delta m^2_{21}>7.5\times10^{-9} \text{ eV}^2. \tag{3.4}$$

Now we choose the range of Δm^2_{21} obtained by Pulido [22] which is consistent with the results of all the four solar neutrino experiments viz.

$$1.3\times10^{-8} \text{ eV}^2<\Delta m^2_{21}<4.6\times10^{-8} \text{ eV}^2. \tag{3.5}$$

For this range of Δm^2_{21}, one can find the ranges in which different categories of neutrinos resonate from Eq. (1.3). Low-energy neutrinos resonate in the range

$$0.5<r/Rs<0.60, \tag{3.6a}$$

whereas the intermediate-energy neutrinos resonate in the range

$$0.62<r/Rs<0.70. \tag{3.6b}$$

For high-energy neutrinos, the resonance is located in the range

$$0.82<r/Rs<0.93. \tag{3.6c}$$

Now we intend to infer the magnetic field distribution within the convective and radiation zones of the Sun which are consistent with different degrees of suppression observed in Homestake, Kamiokande, and Gallium experiments assuming the validity of RSFP mechanism for neutrino flux suppression. The neutrinos, are assumed to be Majorana particles and the vacuum mixing has been assumed to be zero. In order to eliminate the effect of the time variation of the solar neutrino flux with solar magnetic activity, the neutrino flux data pertaining to the same period have been utilized. To be more specific, the following simultaneous results available from Kamiokande [22] and GALLEX [23] from early 1991 to early 1992 are used:

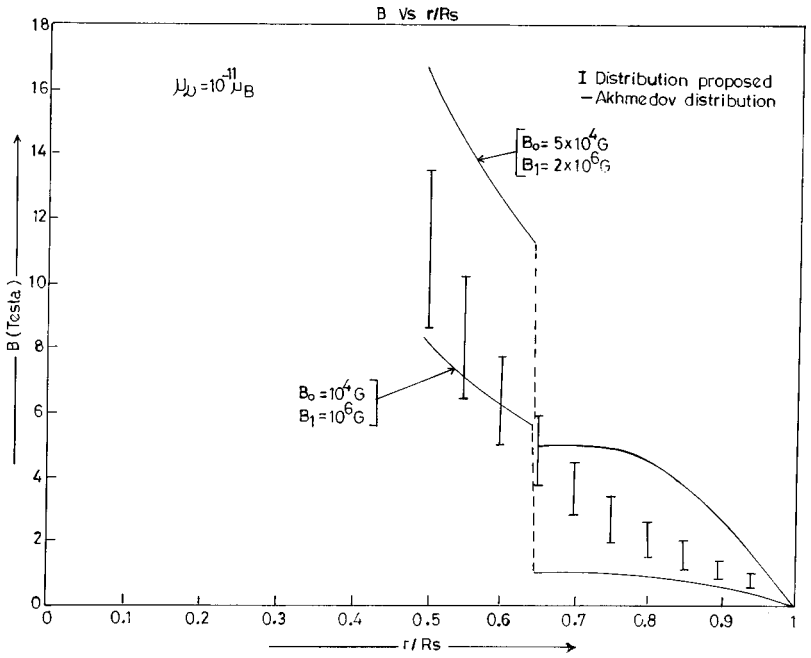

FIG. 6. Distributions of transverse solar magnetic fields.

$$0.59^{+0.11}_{-0.09} \pm 0.06 \ \text{SNU (K III)} \tag{3.7a}$$

and

$$81 \pm 17 \pm 9 \ \text{SNU (GALLEX).} \tag{3.7b}$$

From Homestake [24], an average value

$$2.85 \pm 0.32 \ \text{SNU} \tag{3.7c}$$

pertaining to the period 1986–1992 has been used. These experiments observe very different energy ranges of the solar neutrino spectrum. The GALLEX detects 54% low-energy neutrinos with an average of 0.265 MeV coming from *pp* reactions in the Sun; 35% intermediate energy neutrinos coming predominantly from the ^{7}Be source with an average energy of 0.86 MeV and 11% high-energy ones coming from ^{8}B source with an average energy of 7 MeV. Kamiokande on the other hand, detects only ^{8}B neutrinos via the neutral as well as the charged weak currents whereas ν_μ, ν_τ can only interact via the neutral currents for which the cross section is only about 14% of the total. In the absence of any suppression mechanism, Homestake sees 22% intermediate-energy and 78% high-energy neutrinos. Therefore, for each one of these experiments one has

$$R_{\text{Ga}} = 0.54P_L + 0.35P_I + 0.11P_H, \tag{3.8a}$$

$$P_{\text{K III}} = 0.14 + 0.86P_H, \tag{3.8b}$$

and

$$R_{\text{Homestake}} = 0.22P_I + 0.78P_H, \tag{3.8c}$$

where R denotes the ratio of observed and predicted neutrino fluxes in different solar neutrino experiments. P_L, P_I, and P_H denote the survival probabilities for electronic neutrinos of low-, intermediate-, and high-energy neutrinos defined above. The central values of P_L, P_I, and P_H can be worked out from a knowledge of R_{Ga}, $R_{\text{K III}}$, and $R_{\text{Homestake}}$.

It is clear that RSFP is strongly energy dependent and results in different degrees of suppression and time variation in different solar neutrino experiments. Assuming that the RSFP is responsible for neutrino flux suppression, one can use Eqs. (1.3)–(1.5) to infer the magnetic field distribution consistent with the values of P_L, P_I, and P_H obtained from Eqs. (3.7) and (3.8). The factor $\cos 2\tilde{\theta}_0 \cos 2\tilde{\theta}_1 \sim 1$ for the most expected values of the magnetic field strength in the solar core and the solar surface for the range of Δm^2_{21} mentioned in Eqs. (3.4) and (3.5). The resulting magnetic field distribution is shown in Fig. 6. For a neutrino magnetic moment $\mu_\nu = 10^{-11}\mu_B$. The uncertainties in the value of R are reflected in the form of very large error bars in the radiation zone whereas near the edge the magnetic fields are more sharply defined. The preliminary results of this investigation have been already reported [25].

IV. CONCLUSIONS

It has been shown that all the existing solar neutrino data can be explained within the framework of the RSFP scenario for suitable magnetic field profiles in the Sun. The latest update on neutrino parameters consistent with all the existing solar neutrino data has been obtained. It is expected that further data from the high statistics super-Kamiokande experiment will settle the issue of anticorrelation of solar neutrino flux with solar magnetic activity. Till such time RSFP of neutrinos in solar magnetic fields remains as viable a solution as the elegant MSW mechanism. It has been attempted to constrain solar magnetic fields from solar neutrino observations assuming the RSFP of neutrinos to be responsible for solar neutrino deficit. Solar magnetic field distribution con-

sistent with the results of the ongoing solar neutrino experiments has been obtained and displayed in Fig. 6 along with the Akhmedov distribution. It is clear from this figure that the rate of decrease of the transverse magnetic field in the radiation zone is much faster than that in the convective zone. This is in agreement with the analysis of Babu, Mohapatra, and Rothstein [26] who attempted to reconcile different degrees of time variation of neutrino flux observed in Homestake and Kamiokande. Transverse magnetic field distribution derived in this work is in reasonably good agreement with the magnetic field distribution proposed by Akhmedov [Eq. (2.5)]. Radiation zone magnetic fields obtained in this work are in good agreement with the distribution proposed by Akhmedov for $10^6\,\mathrm{G}<B_1<10^7\,\mathrm{G}$ with the neutrino magnetic moment in the range $3.2\times10^{-13}\mu_B\leqslant\mu_\nu\leqslant5.2\times10^{-11}\mu_B$. The convective zone magnetic fields obtained in this work are in remarkably good agreement with the Akhmedov distribution for $10^4\,\mathrm{G}<B_0<10^5\,\mathrm{G}$ for neutrino magnetic moment in the range $1.5\times10^{-11}\mu_B\geqslant\mu_\nu\geqslant10^{-13}\mu_B$.

The magnitudes of the magnetic field in the radiation and convective zones of the Sun are very sensitive to the value chosen for the neutrino magnetic moment. However, uncertainty in the value of the neutrino magnetic moment does not affect the distribution of the magnetic field. More reliable bounds on the neutrino magnetic moment will be helpful in deciding the exact order of magnetic fields at different points in the solar interior while more reliable bounds on Δm^2_{21} will be helpful in determining the magnetic field distribution in the solar interior more accurately. However, this work completely rules out the magnetic field distribution used by Pulido [12] in the radiation zone. This work was largely inspired by the work of Akhmedov, Lanza, and Petcov [27] which analyzed the then available solar neutrino data within the framework of the RSFP scenario. In particular, they predicted the neutrino detection rates in various ongoing solar neutrino experiments using several magnetic field profiles. They noted that the quality of the data fit is very sensitive to the magnetic field profiles used which led them to mention the possibility of extracting the magnetic field distribution in the solar interior from the solar neutrino data in the framework of the RSFP scenario.

ACKNOWLEDGMENTS

One of the authors (B.C.C.) is thankful to the University Grants Commission, Govt. of India for financial support.

[1] J. N. Bahcall and M. H. Pinsonneault, Rev. Mod. Phys. **64**, 88 (1993).
[2] Particle Data Group, R. M. Barnett *et al.*, Phys. Rev. D **54**, 294 (1996).
[3] L. Wolfenstein, Phys. Rev. D **17**, 2369 (1978); S. P. Mikheyev and A. Yu Smirnou, Sov. J. Nucl. Phys. **42**, 913 (1985).
[4] M. B. Voloshin, M. I. Vysotsky, and L. B. Okun, Sov. J. Nucl. Phys. **44**, 440 (1986); M. B. Voloshin and M. I. Vysotsky, *ibid.* **44**, 544 (1986).
[5] C. S. Lim and W. J. Marciano, Phys. Rev. D **37**, 1368 (1988).
[6] E. K. Akhmedov, Phys. Lett. B **213**, 64 (1988).
[7] Arnab Rai Choudhuri, Bull. Astron. Soc. India **24**, 219 (1996).
[8] D. S. Oakley and B. Herschel, Astropart. Phys. **7**, 297 (1997); D. S. Oakley *et al.*, Astrophys. J. **437**, L63 (1994).
[9] S. Masseti, M. Storini, and N. Iucci, in Proceedings of the 24th ICRC, Rome, 1995 (unpublished), Vol. 4, p. 1243; S. Masseti, M. Storini, and J. Sykora, *ibid.*, p. 1247.
[10] T. Stanev, in Proceedings of the 4th International Topical Workshop ''New Trends in Solar Neutrino Physics,'' edited by V. Berezinsky and G. Fiorentini, Gran Sasso, Italy, 1996 (unpublished), p. 141.
[11] E. Kh. Akhmedov, invited talk at the 4th International Solar Neutrino Conference, Heidelberg, 1997, Report No. IC/97/49.
[12] J. Pulido, Phys. Rep. **211**, 167 (1992).
[13] W. Kwong and S. P. Rosen, Phys. Rev. Lett. **73**, 369 (1994).
[14] E. K. Akhmedov and O. V. Bychuk, Sov. Phys. JETP **68**, 250 (1989).
[15] B. C. Chauhan and S. Dev, J. Phys. Soc. Jpn. **66**, 917 (1997).
[16] J. Pulido, Phys. Rev. D **48**, 1492 (1993).
[17] J. D. Jackson, *Classical Electrodynamics*, 2nd ed. (Wiley, New York, 1975), Chap. 10.
[18] E. N. Parker, *Cosmic Magnetic Fields* (Clarendon, Oxford, 1979).
[19] J. N. Bahcall, *Neutrino Astrophysics* (Cambridge University Press, Cambridge, England, 1989).
[20] J. Schmitt and R. Rosner, Astrophys. J. **265**, 901 (1983).
[21] E. N. Parker, Astrophys. J. **286**, 666 (1984); E. A. Muller *et al.*, Sol. Phys. **41**, 53 (1975); T. Walker *et al.*, Astrophys. J. **376**, 51 (1991).
[22] Kamiokande III Collaboration, K. Nakamura *et al.*, in *Neutrino 92* [Nucl. Phys. B (Proc. Suppl.) **31**, 105 (1993)].
[23] GALLEX Collaboration, P. Anselmann *et al.*, Phys. Lett. B **314**, 445 (1993).
[24] D. Morrison, Report No. CERN-PPE/93-196.
[25] B. C. Chauhan, U. C. Pandey, and S. Dev, Mod. Phys. Lett. A **13**, 1163 (1998).
[26] K. S. Babu, R. N. Mohapatra, and I. Rothstein, Phys. Rev. D **44**, 2265 (1991).
[27] E. K. Akhmedov, A. Lanza, and S. T. Petcov, Phys. Lett. B **303**, 85 (1993).